



Published in final edited form as:

*Pediatr Res.* 2021 July ; 90(1): 58–65. doi:10.1038/s41390-020-01224-5.

## Short exposure to hyperoxia causes cultured lung epithelial cell mitochondrial dysregulation and alveolar simplification in mice

David Garcia<sup>1,7</sup>, Jennifer F. Carr<sup>2,7</sup>, Felix Chan<sup>2</sup>, Abigail L. Peterson<sup>2</sup>, Kimberlyn A. Ellis<sup>2</sup>, Alejandro Scaffa<sup>3</sup>, Andrew J. Ghio<sup>4</sup>, Hongwei Yao<sup>2</sup>, Phyllis A. Dennery<sup>\*,2,5,6</sup>

<sup>1</sup>Department of Chemistry, Brown University, Providence, Rhode Island <sup>2</sup>Department of Molecular Biology, Cell Biology and Biochemistry, Brown University, Providence, Rhode Island <sup>3</sup>Department of Molecular Pharmacology, Physiology, and Biotechnology, Brown University, Providence, Rhode Island <sup>4</sup>US Environmental Protection Agency, Chapel Hill, North Carolina <sup>5</sup>Department of Pediatrics, Warren Alpert Medical School, Brown University, Providence, Rhode Island <sup>6</sup>Hasbro Children's Hospital, Providence, Rhode Island.

### Abstract

**Background:** Prolonged exposure to high oxygen concentrations in premature infants, although lifesaving, can induce lung oxidative stress and increase the risk of developing BPD, a form of chronic lung disease. The lung alveolar epithelium is damaged by sustained hyperoxia, causing oxidative stress and alveolar simplification, however, it is unclear what duration of exposure to hyperoxia negatively impacts cellular function.

**Methods:** Here we investigated the role of a very short exposure to hyperoxia (95% O<sub>2</sub>, 5% CO<sub>2</sub>) on mitochondrial function in cultured mouse lung epithelial cells and neonatal mice.

**Results:** In epithelial cells, 4 hours of hyperoxia reduced oxidative phosphorylation, respiratory complex I and IV activity, utilization of mitochondrial metabolites, and caused mitochondria to form elongated tubular networks. Cells allowed to recover in air for 24 hours exhibited a persistent global reduction in fuel utilization. In addition, neonatal mice exposed to hyperoxia for only 12 hours demonstrated alveolar simplification at postnatal day 14.

**Conclusion:** A short exposure to hyperoxia leads to changes in lung cell mitochondrial metabolism and dynamics, and has a long term impact on alveolarization. These findings may help inform our understanding and treatment of chronic lung disease.

---

Users may view, print, copy, and download text and data-mine the content in such documents, for the purposes of academic research, subject always to the full Conditions of use:[http://www.nature.com/authors/editorial\\_policies/license.html#terms](http://www.nature.com/authors/editorial_policies/license.html#terms)

\*Corresponding author information: Phyllis A. Dennery; Hasbro Children's Hospital, Department of Pediatrics, 593 Eddy St, Providence, RI 02903; phyllis\_dennery@brown.edu; (401) 444-5648.

<sup>7</sup>These authors contributed equally

Acknowledgements and Author Contributions

We are grateful to Dr. Ronald Mason for the generous gift of DMPO antibody. Conception and design: DG, PAD. Acquisition and analysis of data: DG, JFC, FC, ALP, KAE, AS, AJG, HY, PAD. Drafting and revising the paper: DG, JFC, PAD. Final approval of version to be published: DG, JFC, PAD.

**Disclosure statement:** The authors declare that they have no conflicts of interest.

Patient consent was not required for this study.

## Introduction

Many studies have shown that prolonged exposures to supraphysiologic oxygen levels (hyperoxia) lead to oxidative stress and lung alveolar injury (1-3). However, in newborns, even a brief exposure to hyperoxia in the delivery room can be injurious (4,5). Furthermore, whether there are longer term consequences of a short exposure to hyperoxia occurs is not clear.

Type II alveolar epithelial cells (AECs) are responsible for the biosynthesis and secretion of pulmonary surfactant and are progenitors of type I AECs, which serve to facilitate oxygen diffusion into capillaries (6). Type II cells have high energy demands due to their continuous synthesis and release of pulmonary surfactant. Type II cells rely on mitochondria for the production of acetyl-CoA, allowing for the generation of phospholipids (7). Consequently, these cells contain three times the amount of mitochondrial volume per cell than any other lung cell and the number and size of their mitochondria are reduced upon differentiating to Type I AECs (8,9).

Mitochondria form intracellular interconnected dynamic networks, and their shape and size are altered in order to meet cellular metabolic demands (10). Fusing of mitochondrial populations occurs in response to cellular or mitochondrial stress and during normal mitochondrial turnover (10). Cells such as lung microvascular endothelial cells, which are more glycolytic and less dependent on oxidative phosphorylation (oxphos), have mitochondria with a punctate appearance (11). Type II AECs exposed to cytotoxic cigarette smoke, which primarily depend on oxphos, display more fusion and the formation of elongated mitochondrial networks (12).

The mouse lung epithelial cell line MLE-12 expresses pulmonary surfactant proteins B and C and mimics a type II AEC model. It has been shown that MLE cell lines recapitulate type II AEC metabolic phenotypes, specifically with respect to oxygen exposure (13). Previously it was shown that a 24-hour exposure of these cells to hyperoxia reduced overall oxphos as well as the activities of respiratory complexes I and II (14). However, it is not known if a much shorter duration of exposure to high oxygen is sufficient to affect metabolic function. Here we look at the acute effects of MLE-12 cells exposed to 4 hours of hyperoxia (95% O<sub>2</sub>, 5% CO<sub>2</sub>), and at effects sustained with a 24 hour recovery in air (21% O<sub>2</sub>, 5% CO<sub>2</sub>). We found that a short exposure caused dysregulation of glucose utilization and reduced oxphos and ATP production. With a 24 hour recovery, cells sustained metabolic dysregulation and reduced mitochondrial fuel utilization. Furthermore, 4 hours of hyperoxia was sufficient to induce changes in mitochondrial dynamics, although these changes recovered after 24 hours. Additionally, neonatal mice exposed to hyperoxia for as little as 12 hours show lasting alveolar simplification at postnatal day 14 (pnd14).

## Methods

### Cell lines, culture, and hyperoxia.

MLE-12 cells were purchased from ATCC. Cells were cultured in DMEM/F12 media containing 2% FBS, insulin (5µg/mL), transferrin (10 µg/mL), sodium selenite (30nM),

hydrocortisone (10nM),  $\beta$ -estradiol (10nM), HEPES (10nM) and glutamine (2mM). In air, cells were maintained at 37° C (21% O<sub>2</sub>, 5% CO<sub>2</sub>). In the acute model, cells were exposed to 4 hours of hyperoxia (95% O<sub>2</sub>, 5% CO<sub>2</sub>). In the recovery model cells were exposed to 4 hours of hyperoxia (95% O<sub>2</sub>, 5% CO<sub>2</sub>), then placed in air (21% O<sub>2</sub>, 5% CO<sub>2</sub>) for 24 hours.

### **Mouse hyperoxic exposure and lung morphology.**

Newborn C57BL/6J mice (<12 h old) along with their mothers were exposed to room air or hyperoxia (>95% O<sub>2</sub>) for 12 hours or 24 hours in an A-chamber (BioSpherix, Redfield, NY) (15). Pups were allowed to recover in room air until time of harvest. Radial alveolar count (RAC) was measured as described (16). In brief, lungs were perfused with PBS, inflated with 1% low melt agarose in PBS using 100  $\mu$ L/g body weight, fixed with 4% paraformaldehyde and embedded in paraffin. Lungs were sectioned into 5 $\mu$ m sections and stained with hematoxylin and eosin (H&E). A perpendicular line was drawn from the center of a respiratory bronchiole to the nearest connective tissue septum and the number of alveoli intersected by this line was counted as RAC. All animal experiments were reviewed and approved by the Institutional Animal Care and Use Committee of Brown University.

### **Mitochondrial stress test.**

Oxidative phosphorylation was measured using the XF<sup>e</sup>24 Seahorse Bioanalyzer (Agilent) following manufacturer's instructions. In the acute model, cells were seeded in seahorse assay plates 24 hours in air (21% O<sub>2</sub>/ 5 % CO<sub>2</sub>) prior to assay. The day of the assay, cells were exposed to hyperoxia for 4 hours. In the recovery model, cells were exposed to 4 hours of hyperoxia, trypsinized, counted, and seeded in Seahorse plates in air for 24 hours. Immediately prior to the assay cells were confirmed to be evenly seeded and one well from each condition was counted by trypan blue exclusion and used for normalization.

### **Evaluation of electron flow.**

Cells were plated and normalized as above and the XF<sup>e</sup>24 Seahorse Bioanalyzer was used to measure OCR. Activity was assessed in 1x MAS buffer (described in XF Plasma Membrane Permeabilizer Guide (PMP); Agilent) including 10 mM pyruvic acid, 2 mM malate, 4  $\mu$ M FCCP, 4 mM ADP, 0.2% (w/v) fatty acid-free BSA and 1 nM PMP reagent. Final concentrations of injected reagents were: 2  $\mu$ M rotenone, 10 mM succinate, 1.5  $\mu$ g/ mL antimycin A, 10 mM ascorbate, and 100  $\mu$ M tetramethyl-*p*-phenylenediamine (TMPD).

### **Metabolic pathway analysis.**

Cells were harvested after exposures and resuspend in 1x MAS buffer. Cells were filtered through a 70-micron nylon filter (cell strainer, Falcon 352350) to remove clumps. Cells were counted to determine their viability with trypan blue. The cells had viability >95%. According to manufactures instructions (Biolog), 30 $\mu$ l per well of the Assay Mix were pipetted into all wells and incubate at 37°C for 1 hour to allow substrates to fully dissolve, followed by addition of 30  $\mu$ l cell suspension to all wells. The MitoPlate was read for 4 hours at OD590 on a microplate reader in kinetic mode.

### **Iron measurement.**

Non-heme iron concentrations were quantified using inductively coupled plasma optical emission spectroscopy (Model Optima 4300D, Perkin Elmer, Norwalk, CT) operated at wavelengths of 238.204 and 259.939 nm.

### **Determination of steady state mRNA levels.**

Total RNA was isolated by using the RNeasy kit (Qiagen). Reverse transcription was performed with MultiScribe reverse transcriptase (Invitrogen). Taqman Universal PCR Master Mix and Taqman probes were from ThermoFisher: Opa1 (Mm01349707), Mfn1 (Mm00612599), Mfn2 (Mm00500120), Dnm1 (Mm01342903), Drp1 (Mm01342903), MTP18 (Mm00466042), Fis1 (Mm00481580), PPAR $\gamma$  (Mm01184322), PGC1 $\alpha$  (Mm01208835), TFAM (Mm00447485), TIM23 (Mm03010822), HO-1 (Mm00516006)

### **Determination of protein levels and activity.**

Western blotting was used to measure relative protein levels as previously described (17). Briefly, protein lysates were run on a 4-12% sodium dodecyl sulfate polyacrylamide gel (Invitrogen) and transferred to a PVDF membrane, which were incubated with the following primary antibodies: TOM20 (Cell Signaling 42406s), transferrin receptor (ThermoFisher 13-6800), ferritin (ab75973), DMPO was a kind gift of Ron Mason. Appropriate horseradish peroxidase conjugated secondary antibodies were used for visualization with Luminata Crescendo (EMD Millipore) or SuperSignal West Femto substrate (ThermoFisher) using the ChemiDoc Touch Imaging System (BioRAD). The in-gel aconitase activity was conducted as described (18).

### **Proliferation Assays.**

To examine proliferation, cells were labeled with 5-ethynyl-2'-deoxyuridine (EdU) Alexa Fluor 488 (C10425, ThermoFisher) according to instructions. For viability, cells were labeled with Propidium iodide (P1304MP, ThermoFisher) according to instructions. Fluorescence intensity was measured using a BD FACSAria flow cytometer and analyzed with FlowJo V10. We seeded 400,000 MLE-12 cells/well in a 6-well plate in triplicate.

### **Super resolution imaging of mitochondria.**

Cells were visualized utilizing Cytiva DeltaVision OMX SR super-resolution microscope system (Cytiva). Structured illumination is an imaging technique that generates super resolved images through the interaction of structured light patterns with sample. Computer algorithms process the collected raw data set and generate the final super-resolution image

### **Fluorescent labeling of mitochondria.**

Cells were labeled with Mitotracker Green FM (M7514, ThermoFisher), MitoTracker RedCMXRos (M7512m ThermoFisher), and TMRM (T668, ThermoFisher) according to instructions. Fluorescence intensity was measured using a BD FACSAria flow cytometer and analyzed with FlowJo V10.

## Statistical Analysis.

All experiments with MLE-12 cells had a minimum of 3 biological replicates. Error bars are reported as the mean  $\pm$  standard error of the mean (SEM) for all values. Graph Pad Prism 6 software was used to do unpaired students t-tests for comparisons between two groups, with a  $p < 0.05$  used as a threshold for significance.

## Results

### Four hours of hyperoxia reduces oxphos in MLE-12 cells

In mouse lung epithelial cells, it was previously shown that 24 hours of hyperoxia reduced oxphos (14) but we wished to know if a shorter exposure would alter metabolism. We used a mitochondrial stress test to measure oxygen consumption rate (OCR) in a Seahorse Bioanalyzer and found a reduction in basal respiration and maximum respiration after 4 hours of hyperoxia compared to air (Figure 1A). Cells exposed to 8 hours of hyperoxia had a further reduction in basal and maximal respiration, demonstrating a dose-dependency (Supplementary Figure 1). The reduction in oxphos at 4 hours was associated with dysregulated energy production, as the Seahorse ATP production assay showed a reduction in the total amount of ATP generated and ATP produced by mitochondria (Figure 1B). We next utilized a glycolytic rate assay (GRA), which measures the glycolytic proton efflux rate, to examine glycolysis. We found no changes in basal glycolysis or the glycolytic response to inhibition of oxphos, termed compensatory glycolysis, indicating that 4 hours of hyperoxia does not alter glycolysis (data not shown).

We wondered if the reduced oxphos observed with 4 hours of hyperoxia changes the activity of complexes in the electron transport chain (ETC). Using permeabilized cells, we interrogated various ETC complexes as illustrated schematically (Figure 1C). The flow of electrons from complex I through IV is halted at CI by administration of rotenone, followed by the regeneration of electron flow at CII with injection of succinate. Electron flow is stopped at CIII by antimycin A but is then resumed by administration of TMPD/ ascorbate to determine function of complex IV. We found that cells exposed to 4 hours of hyperoxia exhibited reduced electron flow at complex I and complex IV (Figure 1C).

We also used a different assay to assess mitochondrial function, the Biolog MitoPlate. This assay can measure oxidation of individual substrates and electron transport chain function with a colorimetric assay. We show that in the absence of any exogenous substrates, the utilization of endogenous substrates was reduced significantly in cells exposed to hyperoxia (Figure 1D). Since mitochondrial function is vital in maintaining global cellular processes, we also examined cell proliferation and viability. However, we found no change in proliferation, measured by EdU incorporation, and no change in viability, measured by propidium iodide incorporation/ exclusion, with 4 hours hyperoxia (Figure 1E, F).

### Some metabolic defects persist with 24 hours of recovery

To determine whether the effects observed at 4 hours persisted, we exposed MLE-12 cells to hyperoxia and allowed them to recover in air for 24 hours and examined metabolism. Glycolysis was still unchanged in recovery (data not shown). In the mitochondrial stress

test OCR returned to baseline, as indicated by no change in basal respiration or maximum respiration (Supplementary Figure 2A). Equally, changes in electron flow seen acutely at 4 hours were now restored with 24 hours of air recovery and there was still no effect on cell proliferation or viability (Supplementary Figure 2B-D).

In order to expand our understanding of the observed metabolic defects we conducted two distinct assays to better understand mitochondrial fuel utilization, both acutely and with air recovery. The Seahorse fuel utilization assay examines glucose, glutamine and fatty acid consumption; we found that cells exposed to 4 hours hyperoxia had reduced utilization of glucose only (Figure 2A), but that in recovery cells had reduced utilization of all three fuels (Figure 2B). Using the Biolog MitoPlate we also saw acute reduction of glucose ( $\alpha$ -D-glucose) utilization, and reduction in use of downstream glycolytic intermediates D-glucose-6-PO<sub>4</sub> and pyruvic acid, as well as TCA substrate citric acid (Figure 2C). Reduction in utilization of these substrates persisted with 24 hours air recovery (Figure 2D). In addition, specifically in recovery, we saw reduced utilization of TCA cycle intermediates cis-aconitic acid, isocitric acid,  $\alpha$ -keto-glutaric acid and amino acids, including glutamine, and ketone bodies (Supplementary Figure 3). Additionally the mitochondrial utilization of endogenous substrates assessed with the Biolog plate remained reduced (Figure 2E) as did the amount of total ATP production and ATP from mitochondria (Figure 2F).

### Short hyperoxic exposure is not sufficient to induce widespread oxidative damage

High levels of oxygen have been shown to cause damage to macromolecules and to dysregulate cellular processes including metabolism (19-21). Previous studies have focused on the role of oxidative stress in the deleterious effects of hyperoxia on mitochondria (22-25). Thus we wished to examine various markers of oxidative stress after 4 hours hyperoxia and in recovery. We examined superoxide production in live cells with MitoSOX Red staining and FACS analysis and saw no difference at 4 hours (Figure 3A). We looked at protein nitro adducts using a DMPO spin trap antibody, and saw no differences acutely or in recovery (Figure 3A). Equally we saw no changes in expression of the antioxidant response protein HO-1, nor mitochondrial superoxide dismutase (Figure 3A).

Our substrate utilization results indicated a reduction in mitochondrial utilization of citric acid, which is catalyzed by mitochondrial aconitase. Aconitases can serve as oxygen sensors, as their activities depend on iron-sulfur clusters which are particularly sensitive to disruption by oxygen (26). Using an in-gel aconitase assay, which distinguishes cytosolic from mitochondrial aconitase, we saw no change at 4 hours hyperoxia in mitochondrial aconitase activity but did see reduction of cytosolic aconitase (Figure 3B). Cytosolic aconitase activity returned to baseline in recovery (data not shown). To explore the potential role of disrupted iron homeostasis after 4 hours exposure, we examined levels of the iron storage protein ferritin and found it was reduced, while the levels of iron importer transferrin receptor were unchanged (Supplementary Figure 4A,B). This raised the possibility that iron might be limiting so we measured total cellular non-heme iron, but found no difference between air and 4 hours hyperoxia (Supplementary Figure 4C).

In order to evaluate mitochondrial membrane potential, we stained cells with tetramethylrhodamine methyl ester (TMRM) found no reduction in fluorescence by FACS

either after 4 hours hyperoxia or in recovery (Supplementary Figure 5A). As measured by Seahorse OCR in the mitochondrial stress test we also do not see any changes in proton leak indicating mitochondria are not depolarized (Supplementary Figure 5B). We wanted to determine if there was decreased mitochondrial biogenesis, which could explain the observed reduction in oxphos. We found that expression levels of mitochondrial biogenesis transcription factors, TFAM, PGC1 $\alpha$  and PPAR $\gamma$ , all remained unchanged after 4 hours of hyperoxia and in recovery (Supplementary Figure 6A). We also examined levels of mitochondrial membrane proteins TIMM23 and TOMM20 acutely and in recovery as a proxy for the number of mitochondria, and these remain unchanged (Supplementary Figure 6B)

### Short hyperoxic exposure alters mitochondrial morphology

Others have demonstrated that a 6 hour hyperoxic exposure is sufficient to cause mitochondrial fragmentation (27). We wanted to determine if our shorter exposure to hyperoxia would similarly dysregulate mitochondrial dynamics. We found an increase in mRNA levels of fusion proteins *Mfn1* and *Opal* acutely but these returned to baseline in recovery (Figure 4A). No changes in gene expression of fission proteins *Drp1*, *Fis1*, or *Mtp18* were observed acutely, but we saw decreased expression of these proteins in recovery, possibly indicating a protective response in recovery (Figure 4B). To address whether hyperoxia induces mitochondrial mass changes, we utilized MitoTracker Green stain and measured fluorescent signal by FACS. We observed increased fluorescence suggesting an increase in mitochondrial mass of cells exposed to 4 hours of hyperoxia, which then returned to baseline in recovery (Figure 4C).

Next we performed structured illumination microscopy (SIM) to examine mitochondrial morphology with MitoTracker Red CMXRos. In air controls, mitochondria appeared as discrete spheroid organelles that are distributed densely in the perinuclear area (Figure 5A-D). Upon exposure to 4 hours of hyperoxia, the cells demonstrated significant changes in mitochondrial morphology and distribution fitting the transcriptional changes in fusion genes. The mitochondria appeared more evenly distributed across the whole cytoplasmic surface and formed highly elongated and interconnected tubular networks, indicative of a fusion process (Figure 5E-H). Finally, mitochondria returned to control level morphology and distribution with perinuclear clustering of discrete mitochondria after 24 hours of air recovery (Figure 5I-L). The increased fusion seen by SIM with 4 hours hyperoxia correlates with the increased mitochondrial mass measurement using FACS (Figure 4C). Increased mitochondrial mass is likely reflective of the mass of 'clusters' of fused mitochondria.

### Neonatal mice exposed to hyperoxia for 12 hours exhibit alveolar simplification.

We show that MLE-12 cells exposed to 4 hours of hyperoxia have metabolic defects that persist with a 24 hour air recovery (Figure 2). We wished to know if the detrimental effects of a short hyperoxic exposure in a single lung cell type would extend to a more physiological model of neonatal chronic lung disease. Thus we exposed neonatal mice to air or hyperoxia for 12 or 24 hours followed by recovery in air until pnd 14. As seen by H&E staining, as few as 12 hours of hyperoxia caused alveolar simplification and increased airspaces (Figure 6A). Radial alveolar counts (RAC) were performed to quantify

diminished alveolar complexity, and indicated that mice exposed to 12 hours of hyperoxia were significantly compromised compared to air controls. (Figure 6B). Twenty four hours of hyperoxia reduced alveolar complexity even further, indicating a dose-dependent response (Figure 6B). Interestingly we observed resolution of alveolar damage at pnd 60 following a 24 hour neonatal hyperoxia exposure (data not shown). Whether a second insult would lead to increased susceptibility to injury is yet to be determined.

## Discussion

In this study MLE-12 cells were used to examine the effects of 4 hours of hyperoxia (95% O<sub>2</sub>, 5% CO<sub>2</sub>) on mitochondrial function. We found that this very short exposure to hyperoxia dysregulated glucose utilization by mitochondria and reduced oxphos and ATP production. Cells allowed to recover in air for 24 hours show sustained metabolic dysregulation and reduced fuel utilization. With 4 hours of hyperoxia we also observed changes in mitochondrial dynamics but this did not persist in recovery. Additionally, we found that as little as 12 hours of exposure of neonatal mice to hyperoxia is sufficient to cause lasting alveolar simplification, which is clinically relevant as there are cases where neonates are briefly exposed to hyperoxia as life-saving measures.

A prior study demonstrated that exposure of MLE-12 cells to hyperoxia for 24 hours did not alter basal glycolysis and we, too, observe no changes at 4 hours (14). That study also demonstrated reduced activity of overall oxphos and of ETC complexes I and II. Here, with 4 hours hyperoxia, we also see reduction of oxphos and reduced activities of complex I and IV. We cannot be sure what accounts for our differences in complex activities but it may be due to duration of exposure. A study using A549 cells exposed to hyperoxia for 24 hours found an increased rate of glucose consumption approximately two- to fourfold relative to the air exposed cells (27). Here we found reduced utilization of glucose and glycolytic metabolites with a 4 hour exposure. Even though MLE-12 cells are immortalized, the differences in our findings may be cell-type specific as carcinoma cells like A549 cells are known to display the Warburg effect, in which glycolysis is used as the main source of energy (28).

Our observation that oxphos is reduced at 4 hours is due to the combined activities of ETC complexes and mitochondrial glucose utilization. In recovery, we observed that glucose utilization remains reduced and that utilization of glutamine and fatty acids was also significantly reduced, demonstrating persistent dysregulation of the TCA cycle. Previous work in our lab indicates that lung endothelial cells exposed to hyperoxia with a 24 hour recovery displayed increased utilization of fatty acids, highlighting possible cell-specific effects of hyperoxia on metabolism (15). The observed reduction in oxphos may also be due in part to defects in TCA cycle enzymes. For example, MLE-12 cells exposed to 24 hours of hyperoxia exhibited reduced activity of several enzymes including  $\alpha$ -ketoglutarate dehydrogenase and succinate dehydrogenase (14). In our study, 4 hours of hyperoxia did not affect the *in vitro* activity of mitochondrial aconitase despite the reduced mitochondrial utilization of citric acid in permeabilized cells. The Biolog MitoPlate assay reflects the combined action of substrate utilization and ETC function, thus if ETC activity is reduced as we observed, then substrate utilization may be reduced as well (Figure 1D). However,



in recovery, as electron flow and oxphos measured by the Seahorse are restored, we saw persistent reduction in oxphos measured by the MitoPlate (Figure 2E). This suggests that ETC function recovers before restoration of mitochondrial fuel utilization. Notably, we did not extend recovery time for cells beyond 24 hours, thus we are limited in understanding how persistent these metabolic changes may be.

After 4 hours of hyperoxia, we saw reduced *in vitro* activity of cytosolic aconitase only. Studies have shown that hydrogen peroxide and superoxide cause dysregulation of cytosolic aconitase activity (26,29). Other studies using primate and rat lungs showed that mitochondrial aconitase activity was reduced by hyperoxia, but no changes were observed for cytosolic aconitase (30,31). Similarly, A549 cells displayed a reduction in mitochondrial aconitase in as short as 3 hours of hyperoxia (30). Our data support the view that aconitases are quite sensitive to oxygen; it appears that cytosolic aconitase activity in MLE-12 cells is disrupted quickly, while the mitochondrial aconitase may be more protected. Since aconitase activity depends on the presence of oxygen-sensitive iron sulfur clusters, we examined whether iron homeostasis was disrupted with 4 hours hyperoxia. Although we found decreased levels of ferritin, we found no difference in the levels of total cellular iron. This does not preclude potential intracellular redistribution of iron, which may warrant further investigation.

The formation of mitochondrial networks that are elongated is promoted by increased fusion or reduced fission, whereas fragmentation is caused by increased fission or reduced fusion. It has been shown that 24 hours of hyperoxia causes mitochondrial fragmentation in pulmonary endothelial cells (27). With our short exposure we observed an increase in transcription of outer and inner membrane fusion proteins *Mfn1* and *Opa1* which was accompanied by increased mitochondrial mass, although protein levels did not change (data not shown). We also found less mRNA for fission markers *Drp1*, *Fis1* and *Mtp18* in recovery. Although we do not fully understand these observations, it is possible that post-translational modifications are involved in regulating fusion and fission activities, as has been shown for Drp1(32). Mitochondrial metabolism is tied to mitochondrial dynamics, and it has been shown that fusion is a protective response to metabolic dysregulation (33). For example, in fibroblasts and B-cells, limited metabolite/nutrient availability results in connected elongated mitochondria (34,35). Here we see that mitochondria are undergoing a temporary fusion process, creating a hyper-elongated tubular network of mitochondria. This morphological change is similar to that seen previously in MLE-12 cells exposed to cigarette smoke extract (36). This indicates that mitochondrial fusion in MLE-12 cells may represent a general morphological change in response to metabolic or environmental stress. However, in that study mitochondrial fusion was associated with an increased metabolic rate (37), whereas in our model, the mitochondrial fusion is found alongside a general reduction in cellular metabolism.

In human microvascular endothelial cells it has been shown that 24 hours of hyperoxia causes a reduction in cell proliferation and viability (38). With our short exposure of MLE-12 cells we do not see changes in proliferation or cell viability. It appears this time point is too early to detect these changes in cell culture, but whether or not 4 hours of hyperoxia might lead to increased susceptibility to a second insult may be worth

considering. Additionally, it is likely that short neonatal hyperoxic exposure reduces lung cell proliferation and/ or viability, as we observed significant loss of alveolar complexity in mice exposed to 12 hours of hyperoxia, which was exacerbated with 24 hours of exposure. As alveolar simplification was resolved by pnd 60, one limitation of our study is that we do not have a detailed picture of the timeline of recovery, nor of injury to specific cell types. Equally, the extent of injury is expected to be dose-dependent, such that concentrations of oxygen less than the 95% used here would be less deleterious and may resolve on a shorter timeline. Another limitation of this study is that we do not know if the observed lung morphological changes are associated with lung metabolic alterations. It would be of interest to examine ATP production and mitochondrial fuel utilization in the lung, especially since understanding this may present the opportunity to attenuate lung injury with nutritional or metabolic interventions.

## Supplementary Material

Refer to Web version on PubMed Central for supplementary material.

## Acknowledgments

**Statement of financial support:** Research reported in this publication was supported by the National Heart, Lung, and Blood Institute (NHLBI) of the National Institutes of Health under award number HL139080 (to DG), NIH T32 HL134625 (to DG), the Institutional Development Award (IDeA) from the NIGMS of NIH under grant #P20GM103652 (to HY), the Falk Medical Research Trust Catalyst Award (to HY), and the Warren Alpert Foundation at Brown University (to PAD).

## References

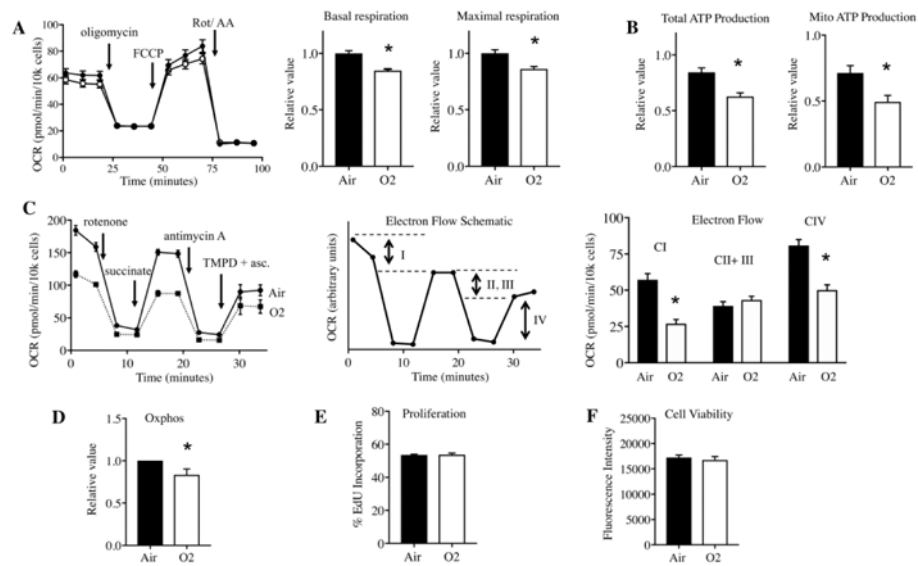
1. Nardiello Cet al. (2017) Standardisation of oxygen exposure in the development of mouse models for bronchopulmonary dysplasia. *Dis Model Mech*, 10, 185–196. [PubMed: 28067624]
2. Saugstad OD (2001) Is oxygen more toxic than currently believed? *Pediatrics*, 108, 1203–1205. [PubMed: 11694702]
3. Vento Met al. (2009) Preterm resuscitation with low oxygen causes less oxidative stress, inflammation, and chronic lung disease. *Pediatrics*, 124, e439–449. [PubMed: 19661049]
4. Khaw KS and Ngan Kee WD (2004) Fetal effects of maternal supplementary oxygen during Caesarean section. *Current opinion in anaesthesiology*, 17, 309–313. [PubMed: 17021570]
5. White LNet al. (2017) Achievement of saturation targets in preterm infants <32 weeks' gestational age in the delivery room. *Arch Dis Child Fetal Neonatal Ed*, 102, F423–f427. [PubMed: 28302696]
6. Wang Yet al. (2018) Pulmonary alveolar type I cell population consists of two distinct subtypes that differ in cell fate. *Proceedings of the National Academy of Sciences*, 115, 2407.
7. Ray NBet al. (2010) Dynamic regulation of cardiolipin by the lipid pump Atp8b1 determines the severity of lung injury in experimental pneumonia. *Nature Medicine*, 16, 1120–1127.
8. Budinger GRet al. (2011) Epithelial cell death is an important contributor to oxidant-mediated acute lung injury. *American journal of respiratory and critical care medicine*, 183, 1043–1054. [PubMed: 20959557]
9. Nabhan AN, Brownfield DG, Harbury PB, Krasnow MA and Desai TJ (2018) Single-cell Wnt signaling niches maintain stemness of alveolar type 2 cells. *Science (New York, N.Y.)*, 359, 1118–1123.
10. Mishra P and Chan DC (2014) Mitochondrial dynamics and inheritance during cell division, development and disease. *Nature Reviews Molecular Cell Biology*, 15, 634–646. [PubMed: 25237825]

11. Mishra P, Carelli V, Manfredi G and Chan David C. (2014) Proteolytic Cleavage of Opa1 Stimulates Mitochondrial Inner Membrane Fusion and Couples Fusion to Oxidative Phosphorylation. *Cell Metabolism*, 19, 630–641. [PubMed: 24703695]
12. Mizumura K et al. (2014) Mitophagy-dependent necroptosis contributes to the pathogenesis of COPD. *The Journal of Clinical Investigation*, 124, 3987–4003. [PubMed: 25083992]
13. Lottes RG, Newton DA, Spyropoulos DD and Baatz JE (2014) Alveolar type II cells maintain bioenergetic homeostasis in hypoxia through metabolic and molecular adaptation. *Am J Physiol Lung Cell Mol Physiol*, 306, L947–955. [PubMed: 24682450]
14. Das KC (2013) Hyperoxia Decreases Glycolytic Capacity, Glycolytic Reserve and Oxidative Phosphorylation in MLE-12 Cells and Inhibits Complex I and II Function, but Not Complex IV in Isolated Mouse Lung Mitochondria. *PLOS ONE*, 8, e73358. [PubMed: 24023862]
15. Yao H et al. (2019) Fatty Acid Oxidation Protects against Hyperoxia-induced Endothelial Cell Apoptosis and Lung Injury in Neonatal Mice. *Am J Respir Cell Mol Biol*, 60, 667–677. [PubMed: 30571144]
16. Cooney TP and Thurlbeck WM (1982) The radial alveolar count method of Emery and Mithal: a reappraisal 1—postnatal lung growth. *Thorax*, 37, 572–579. [PubMed: 7179185]
17. Towbin H, Staehelin T and Gordon J (1979) Electrophoretic transfer of proteins from polyacrylamide gels to nitrocellulose sheets: procedure and some applications. *Proc Natl Acad Sci U S A*, 76, 4350–4354. [PubMed: 388439]
18. Tong WH and Rouault TA (2006) Functions of mitochondrial ISCU and cytosolic ISCU in mammalian iron-sulfur cluster biogenesis and iron homeostasis. *Cell Metab*, 3, 199–210. [PubMed: 16517407]
19. McGrath-Morrow SA, Cho C, Soutiere S, Mitzner W and Tuder R (2004) The effect of neonatal hyperoxia on the lung of p21Waf1/Cip1/Sdi1-deficient mice. *Am J Respir Cell Mol Biol*, 30, 635–640. [PubMed: 14607813]
20. McGrath-Morrow SA and Stahl J (2001) Apoptosis in Neonatal Murine Lung Exposed to Hyperoxia. *American Journal of Respiratory Cell and Molecular Biology*, 25, 150–155. [PubMed: 11509323]
21. O'Reilly M and Thebaud B (2014) Animal models of bronchopulmonary dysplasia. The term rat models. *American journal of physiology. Lung cellular and molecular physiology*, 307, L948–958. [PubMed: 25305248]
22. Farrow KNet et al. (2012) Brief hyperoxia increases mitochondrial oxidation and increases phosphodiesterase 5 activity in fetal pulmonary artery smooth muscle cells. *Antioxidants & redox signaling*, 17, 460–470. [PubMed: 22229392]
23. Farrow KNet et al. (2010) Mitochondrial oxidant stress increases PDE5 activity in persistent pulmonary hypertension of the newborn. *Respiratory physiology & neurobiology*, 174, 272–281. [PubMed: 20804862]
24. Ratner V, Sosunov SA, Niatetskaya ZV, Utkina-Sosunova IV and Ten VS (2013) Mechanical ventilation causes pulmonary mitochondrial dysfunction and delayed alveolarization in neonatal mice. *Am J Respir Cell Mol Biol*, 49, 943–950. [PubMed: 23980609]
25. Waxman AB and Kolliputi N (2009) IL-6 protects against hyperoxia-induced mitochondrial damage via Bcl-2-induced Bak interactions with mitofusins. *American journal of respiratory cell and molecular biology*, 41, 385–396. [PubMed: 19168699]
26. Gardner PR, Raineri I, Epstein LB and White CW (1995) Superoxide radical and iron modulate aconitase activity in mammalian cells. *The Journal of biological chemistry*, 270, 13399–13405. [PubMed: 7768942]
27. Ma C et al. (2018) Hyperoxia Causes Mitochondrial Fragmentation in Pulmonary Endothelial Cells by Increasing Expression of Pro-Fission Proteins. *Arteriosclerosis, Thrombosis, and Vascular Biology*, 38, 622–635.
28. Allen CB and White CW (1998) Glucose modulates cell death due to normobaric hyperoxia by maintaining cellular ATP. *The American journal of physiology*, 274, L159–164. [PubMed: 9458814]
29. Pantopoulos K and Hentze MW (1995) Rapid responses to oxidative stress mediated by iron regulatory protein. *The EMBO journal*, 14, 2917–2924. [PubMed: 7796817]

30. Gardner PR, Nguyen DD and White CW (1994) Aconitase is a sensitive and critical target of oxygen poisoning in cultured mammalian cells and in rat lungs. *Proc Natl Acad Sci U S A*, 91, 12248–12252. [PubMed: 7991614]
31. Morton RL, Iklé D and White CW (1998) Loss of lung mitochondrial aconitase activity due to hyperoxia in bronchopulmonary dysplasia in primates. *American Journal of Physiology-Lung Cellular and Molecular Physiology*, 274, L127–L133.
32. Wang ZW et al. (2020) Mitochondrial Fission Mediated Cigarette Smoke-induced Pulmonary Endothelial Injury. *American journal of respiratory cell and molecular biology*.
33. Yao C-H et al. (2019) Mitochondrial fusion supports increased oxidative phosphorylation during cell proliferation. *Elife*, 8, e41351. [PubMed: 30694178]
34. Gomes LC, Di Benedetto G and Scorrano L (2011) During autophagy mitochondria elongate, are spared from degradation and sustain cell viability. *Nature cell biology*, 13, 589–598. [PubMed: 21478857]
35. Molina AJA et al. (2009) Mitochondrial networking protects beta-cells from nutrient-induced apoptosis. *Diabetes*, 58, 2303–2315. [PubMed: 19581419]
36. Ballweg K, Mutze K, Königshoff M, Eickelberg O and Meiners S (2014) Cigarette smoke extract affects mitochondrial function in alveolar epithelial cells. *American Journal of Physiology-Lung Cellular and Molecular Physiology*, 307, L895–L907. [PubMed: 25326581]
37. Meiners S and Ballweg K (2014) Proteostasis in pediatric pulmonary pathology. *Molecular and cellular pediatrics*, 1, 11. [PubMed: 26567105]
38. Attaye I et al. (2017) The effects of hyperoxia on microvascular endothelial cell proliferation and production of vaso-active substances. *Intensive Care Med Exp*, 5, 22–22. [PubMed: 28409476]

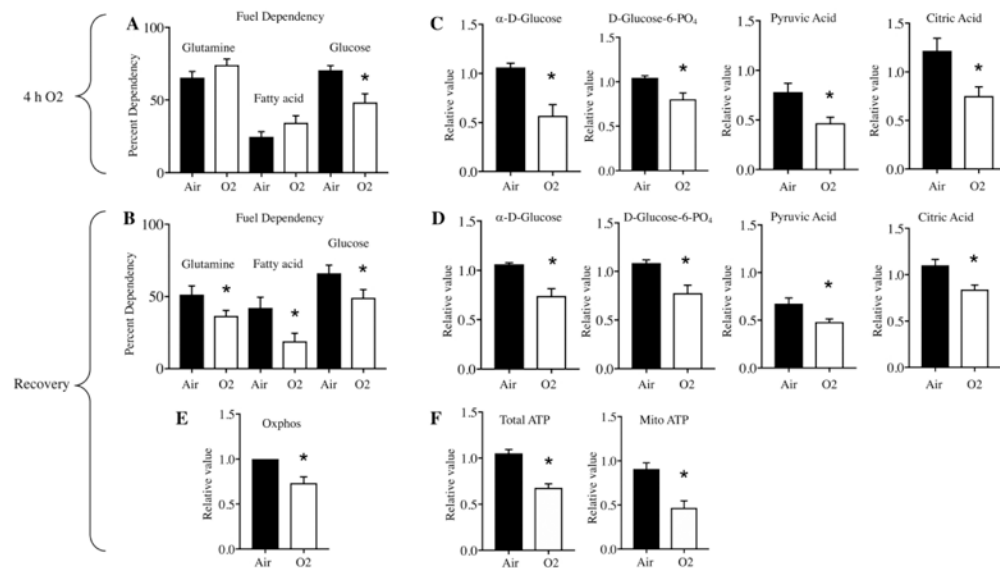
**Impact:**

- Many studies use long exposures (up to 14 days) to hyperoxia to mimic neonatal chronic lung disease.
- We show that even a very short exposure to hyperoxia leads to long term cellular injury in Type II-like epithelial cells.
- This study demonstrates that a short (4 hour) period of hyperoxia has long term residual effects on cellular metabolism.
- We show that neonatal mice exposed to hyperoxia for a short time (12 hours) demonstrate later alveolar simplification.
- This work suggests that any exposure to clinical hyperoxia leads to persistent lung dysfunction.

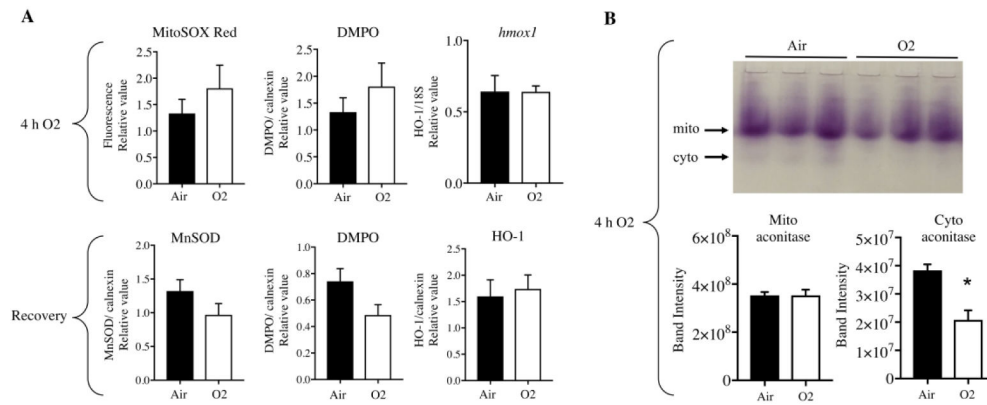


**Figure 1:**

Four hours of hyperoxia is sufficient to cause dysregulation of oxphos, ETC, and energy production. A, Oxygen consumption rate (OCR) was measured with the Seahorse mitochondrial stress test; a representative trace is shown. Basal and maximal respiration were determined according to the manufacturer's instructions. B, Production of total and mitochondrial ATP were measured with the Seahorse ATP rate assay. C, Activity of electron transport chain complexes was determined by a Seahorse electron flow assay. D, Oxidative phosphorylation was determined via the Biolog MitoPlate. E, Cell proliferation was measured by EdU incorporation and FACS analysis. F, Cell viability measured by propidium iodide inclusion/exclusion and FACS analysis. Closed bars represent air exposed cells, and open bars represent cells exposed to hyperoxia for 4 hours. \* $p < 0.05$  vs Air.

**Figure 2:**

Four hours of hyperoxia causes a persistent reduction in fuel utilization. A,B, Dependencies for glutamine, fatty acid, and glucose were measured by the Seahorse fuel utilization assay. C, D, Utilization of glycolytic and tricarboxylic acid (TCA) cycle metabolites were determined by the Biolog MitoPlate. E, Oxidative phosphorylation with 24 h recovery was determined via Biolog MitoPlate. F, Production of total and mitochondrial ATP with 24 h recovery was measured with the Seahorse ATP rate assay. Cells were grown in air (closed bars) or 4 hours of hyperoxia (open bars) (A,C) followed by 24 hours air recovery (B,D,E,F). \* $p < 0.05$  vs Air.

**Figure 3:**

Four hours of hyperoxia does not cause oxidative stress or depolarization of mitochondria.

A, Oxidative stress at 4 hours hyperoxia was determined by measuring the fluorescence signal of MitoSox Red using FACS; 5,5-Dimethyl-1-pyrroline N-oxide (DMPO) reactive oxygen species adducts by Western blot; and heme oxygenase 1 (hmx1) by Taqman.

Oxidative stress with 24 hours recovery was examined by Western blot for manganese superoxide dismutase (MnSOD), DMPO and HO-1. B, Aconitase activity at 4 hours of hyperoxia was measured utilizing an in-gel aconitase assay, loading 65  $\mu$ g lysate per lane. Closed bars represent air exposed cells and open bars represent cells exposed to hyperoxia for 4 hours acutely or with 24 h recovery, as indicated. \* $p < 0.05$  vs Air.



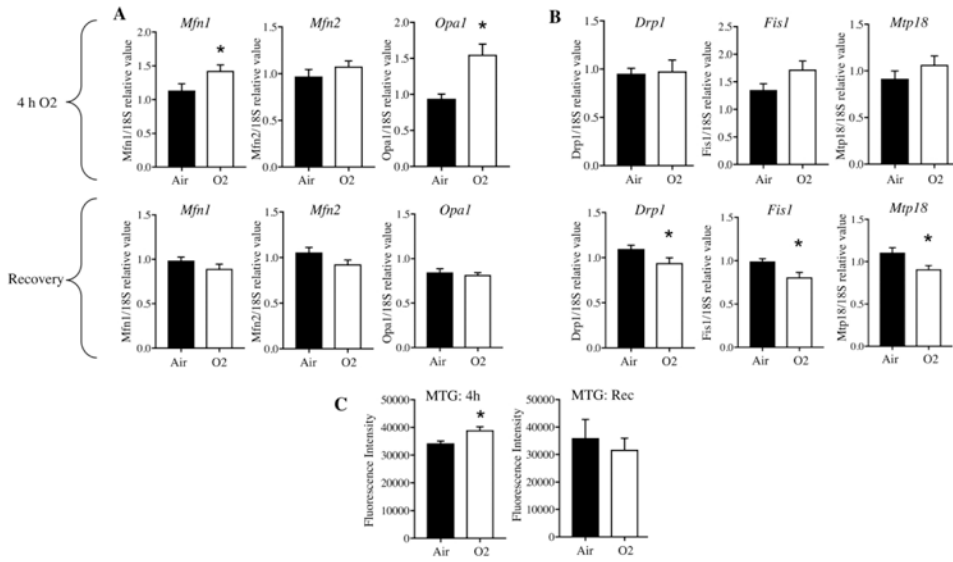


**Figure 4:** Four hours of hyperoxia causes an increase in expression of fusion proteins and mitochondrial mass which does not persist in recovery. A, Gene expression of fusion proteins (Mfn1, Mfn2, Opa1) measured by Taqman acutely (top) and with 24 hours recovery (bottom). B, Gene expression of fission proteins (Drp1, Fis1, Mtp18) measured by Taqman acutely (top) and with 24 hours recovery (bottom). C, Mitochondrial mass was determined by measuring the fluorescence signal of MitoTracker Green (MTG) using FACS at 4h and with 24 h recovery (rec). Closed bars represent air exposed cells and open bars represent cells exposed to hyperoxia for 4 hours acutely or with 24 h recovery as indicated. \* $p < 0.05$  vs Air.

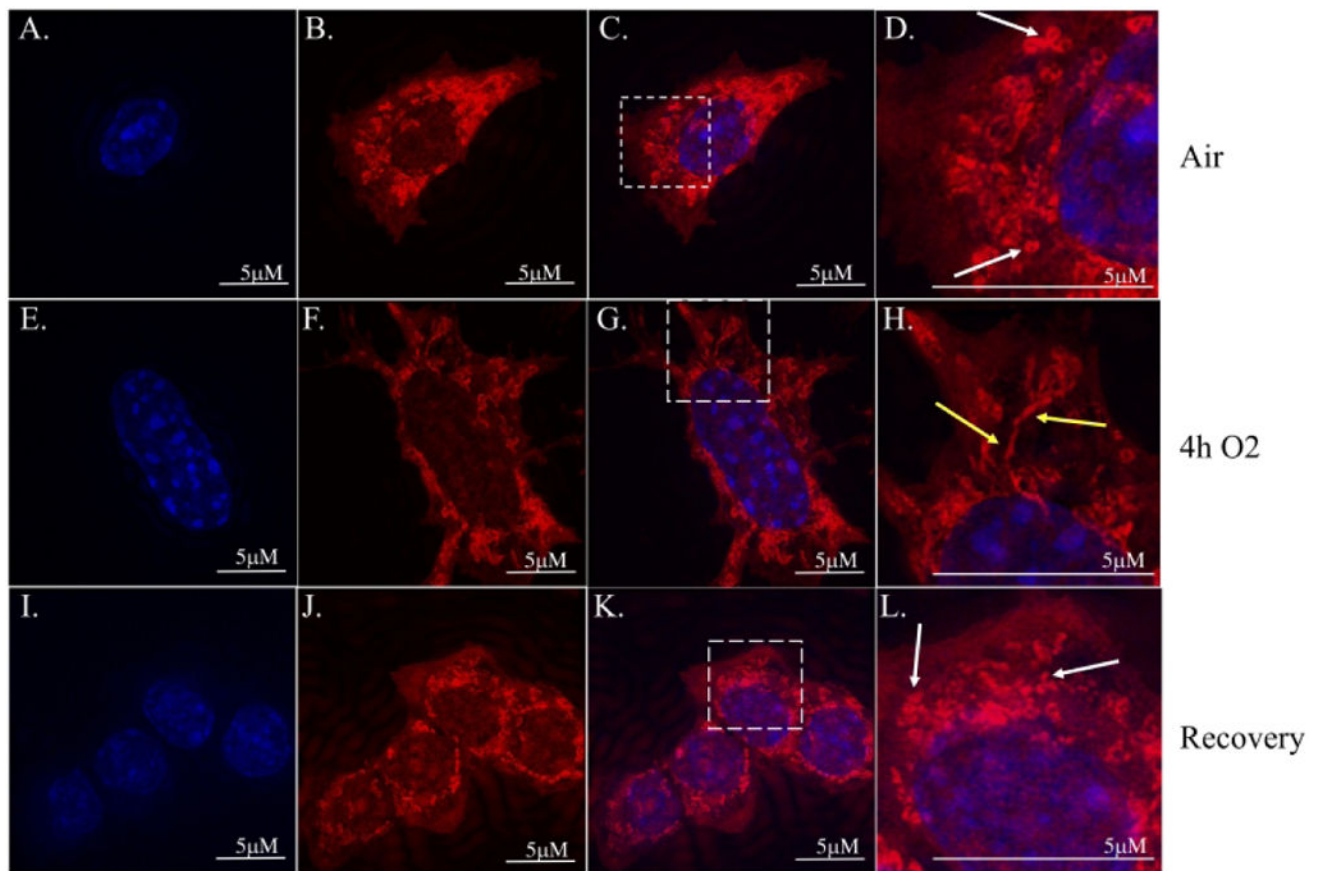


**Figure 5:**

Four hours of hyperoxia causes mitochondria to form elongated interconnected networks which does not persist in recovery. A-D Images of air control cells stained with 4',6-diamidino-2-phenylindole (DAPI (A)) and MitoTracker Red CMXRos (B). C, merged image and D, magnified image of dotted box in C. D, white arrows show round mitochondrial morphology. E-H, Images of cells exposed to 4 hours hyperoxia, and displayed as A-D. H, yellow arrows show elongated interconnected mitochondrial networks. I-L, Images of cells exposed to 4 hours of hyperoxia followed by 24 hours recovery, and displayed as A-D. L, white arrows show round mitochondrial morphology.

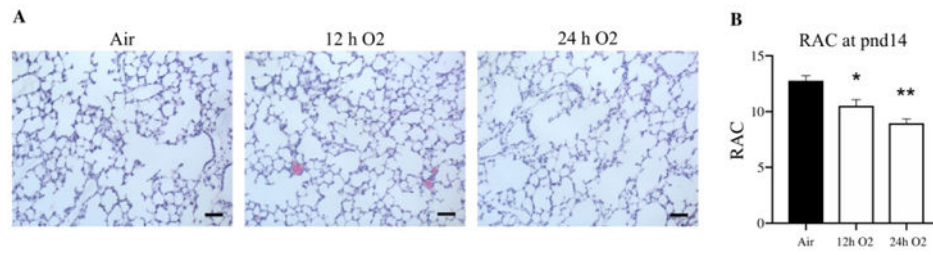


**Figure 6.**

Neonatal short-term hyperoxic exposure impairs mouse lung growth. C57BL/6J neonatal mice (<12 h old) were exposed to air or hyperoxia (95% O<sub>2</sub>) for 12h or 24 h. Mice were allowed to recover in room air until pnd14. A, Representative images of lung tissues stained with H&E. Bar size: 100  $\mu$ m. B, Radial alveolar counts (RAC) were assessed in mouse lungs after mice were exposed to air or hyperoxia for 12 h or 24 h as neonates. N=5-7. \*p<0.05 vs air; \*\*p<0.05 vs 12 h O<sub>2</sub>.